Practical Implementation of a Maximum Power Point Tracker based Improved Sliding Mode Control for Photovoltaic System

Abdelhakim Belkaid,[1,2,3] Jean-Paul Gaubert,[2]
Ahmed Gherbi [3]

[1]Department of Electromechanics, University of Bordj Bou Arreridj, El-Anasser 34030, Bordj Bou Arreridj, Algeria (Tel: 33-(0)751282309; e-mail: belkaid08@yahoo.fr).
[2]Laboratory of Information Technology and Automatic control for the Systems- LIAS ENSIP, Bat B25, 2 rue Pierre Brousse, BP 633, 86022 Poitiers, France (e-mail: jean.paul.gaubert@univ-poitiers.fr)
[3]Automatic Laboratory of Setif (LAS), University of Setif 1, El Maabouda, Street of Bejaia, 19000 Setif, Algeria (e-mail: gherbi_a@univ-setif.dz)

Abstract: Tracking the maximum power point (MPP) has a great interest in the study of photovoltaic (PV) systems. This task is very difficult due to the non linearity of PV current-voltage characteristics which are dependent on the temperature and irradiation conditions. The sliding mode control (SMC) based MPPT with two different step sizes designed for Boost-type DC/DC converter method is investigated in this paper. The robustness of the proposed controller is tested under rapidly changing solar radiations. The SMC based MPPT is compared to perturb and observe (P&O) method and to incremental conductance (IncCond) method. The PV-MPPT system is simulated by Matlab/Simulink environment and verified by practical implementation within DS1104 R&D controller board. The simulation and experimental results are satisfactory and demonstrate that the new SMC can follow the PV peak power at different operating conditions with best performance.

Keywords: Photovoltaic; dSPACE controller board; Maximum power point tracking; Sliding mode control based MPPT; Boost converter.

1. INTRODUCTION

Direct conversion of the sun’s radiation into electrical energy using semiconducting materials is known under the name of photovoltaic effect. Materials presently used for photovoltaic include mono-crystalline silicon, polycrystalline silicon, and amorphous silicon. Unfortunately, these materials exhibit low efficiency in energy conversion. The PV output power generation is influenced by climatic conditions (e.g. irradiance, panel temperature) and load variation.

Therefore a maximum power point tracking (MPPT) technique which is intended to control the DC/DC converter duty cycle is required to ensure an optimal operation of the PV array at different operating conditions (Bratcu, 2008). An overview of more than thirty of these MPPT techniques is done in (Palavee, 2013). Other review articles (Eltawil, 2013; Esram, 2007; Salas, 2006; Subudhi, 2012) give the detailed review of the existing MPPT methods. Among these methods, perturb and observe (P&O) (Femia, 2005; Azzouzi, 2013) and incremental conductance (IncCond) (Dhar, 2013; Safari, 2011) are widely used in the literature, but they fail under fast varying climatic conditions (Ghassami, 2013). The P&O method consists on perturbing the PV output voltage and observing the PV output power to determine the direction of the peak power. The IncCond method tracks the MPP by comparing the instantaneous to the incremental conductance. There are also other techniques such as, fractional short circuit current method (Kollimalla, 2013) which estimates the optimal current by short circuit current and fractional open circuit voltage method (Murtaza, 2012) which estimates the optimal voltage by open circuit voltage. The last two methods are very simple, but they have a weaker and less accurate performance. Reference (Petreus, 2010) compares between four MPPT algorithms which are: fixed step P&O, variable step P&O, incremental conductance and fuzzy logic.

The SMC is mostly used to control the power electronic converters which constitute a case of variable structure systems (Guldemir, 05). Recently, this method is used in photovoltaic systems (Bianconi, 2011; Bianconi, 2013, Komurcugil, 2012) but it is often used to regulate a reference grandeur obtained with another technique such as P&O or IncCond which make the system more complex. This paper proposes SMC based MPPT not to control but to optimize the PV array yield. It is organized as follows, section 2 and 3 provides a modeling of PV array and boost converter, respectively. In section 4, basics of MPPT algorithms are illustrated: P&O, IncCond, and SMC. Thereafter, section 5 and 6 depicts the results of simulations and experiments respectively. Finally, some conclusions are presented in the end of the paper.

2. MATHEMATICAL MODEL OF THE PV ARRAY

Solar cell is the elementary component which converts directly the sun light into electricity. It can produce approximately 2 Watts under 0.5 Volts. The PV cell equivalent electrical circuit adopted in this study is the one diode model (Azzouzi, 2013; Besheer, 2014; Gergaud, 2002; Jamri, 2010) as shown in fig. 1. The single diode model is the most classical model described in the literature, it includes a current generator to model the incident luminous flux, one diode for the polarization phenomena of the cell, a series resistance representing the various contacts and connections resistances, and a shunt resistance characterizing the various leakage currents due to the diode and to the edge effects of the junction.

Thus the mathematical PV array model is given by equation (1) as in (Yu, 2004).

$$I_{pv} = N_p\, I_{ph} - N_p\, I_s \left[exp\left(\frac{V_{pv}+\left(\frac{N_s}{N_p}\right)R_s\, I_{pv}}{n_s a\, v_t}\right)-1\right] - \frac{V_{pv}+\left(\frac{N_s}{N_p}\right)R_s\, I_{pv}}{\left(\frac{N_s}{N_p}\right)R_p} \qquad (1)$$

where N_s and N_p are the number of PV modules connected in series and parallel, respectively; n_s is the number of PV cells connected in series in one module, I_{pv} is the PV array output current, V_{pv} is the PV array output voltage, R_s and R_p are respectively the PV cell series and parallel resistances, a is the ideality factor.

The photo-current I_{ph} depends on the solar irradiance G and temperature T as given in the following equation:

$$I_{ph} = [I_{sc}^{*} + k_i(T - T^{*})]\,\frac{G}{G^{*}} \qquad (2)$$

with k_i is the short circuit current temperature coefficient, $I_{sc}{}^{*}$ is the short circuit current at standard test conditions (STC) which are solar irradiance G^{*} of 1000 W/m^2 (1 sun) at spectral distribution of AM 1.5 and cell temperature T^{*} of 298 Kelvin.

Moreover, the reverse saturation current I_s is calculated using

$$I_s = N_p \left[\frac{I_{sc}^{*}+k_i(T-T^{*})}{exp\left(\frac{V_{oc}^{*}+k_v(T-T^{*})}{n_s v_t}\right)-1}\right] \qquad (3)$$

where $V_{oc}{}^{*}$ is the open circuit voltage at STC conditions, k_v is the open circuit voltage temperature coefficient, and $v_t = a\, k_b\, T/q$ is the thermal voltage, $k_b = 1.38065 \cdot 10^{-23}\, J/K$ is the Boltzmann's constant and $q = 1.60218 \cdot 10^{19}\, C$ is the electronic charge.

The MSX-60 Solar Panel from Solarex Manufacturer with specifications presented in table I is used for simulations and experiments. Fig. 2 shows the power-voltage and the current-voltage characteristics of the PV module under different irradiation levels with fixed temperature (25°C). The same characteristics for a constant irradiance of 1000 W/m^2 and different temperatures are illustrated in fig. 3. These characteristics are achieved using MATLAB simulations with the following parameters $R_s = 0.357\, \Omega$, $R_p = 151\, \Omega$, $n_s = 36$, $a = 1$, $I_{sc}^{*} = 3.8\, A$, $V_{oc}^{*} = 21.1\, V$, $k_v = -0.08\, V/°C$, $k_i = 0.003\, \%/°C$. From these characteristics, it can be seen that the increase of the irradiation or the decrease in temperature increases the power of the panel.

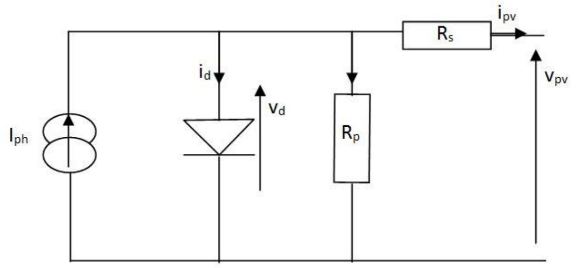

Fig. 1. PV panel electrical model

3. MATHEMATICAL MODEL OF THE DC/DC CONVERTER

The studied system consists on solar energy source coupled to adaptation converters (maximum power point trackers, MPPT). These adapters are DC/DC converters with various topologies. The MPPT DC-DC converter delivers power to DC bus and follows the peak power of photovoltaic panel. They accept a DC input voltage and output a DC voltage higher, lower or the same as the input voltage. Most MPPT trackers are based on buck converter (step-down), boost converter (step-up), buck-boost converter or cuk converter.

These converters use inductors and capacitors to control the energy flow from the solar module to the load by continuously opening and closing a switch. The switch is usually an electronic device (MOSFET or IGBT) that operates in two states: in the conduction mode (on) or in the cut-off mode (off). The non-isolated boost dc–dc converters are widely used in stand-alone photovoltaic power systems because of their simplicity and efficiency (Xiao, 2007).

The non-isolated DC/DC boost converter is inserted to interface the PV output to the rest of the conversion chain as shown in figure 4, not only to adapt the voltage levels but also to track the MPP of the PV array. This converter is widely used in stand-alone PV power systems, It is characterized by its cyclic ratio D $(0 \leq D \leq 1)$, which helps to express the mean values of the output parameters in function of the input ones. If the chopping frequency is sufficiently high compared to the characteristic frequency of the system, the equations governing the step up type DC-DC converter topology using mean values can be written as follows: (Keshri, 2014)

$$\frac{V_0}{V_{pv}} = \frac{I_{pv}}{I_0} = \frac{1}{1-D} \qquad (4)$$

where V_0 and I_0 are the output capacitor voltage and load current, respectively.

In state space form, the dynamic model is obtained as (Radjai, 2014)

$$\begin{cases} \frac{di_L}{dt} = \frac{V_{pv}-V_0}{L} + \frac{V_0}{L}.u \\ \frac{dV_0}{dt} = \left(-\frac{V_0}{RC_2} + \frac{i_L}{C_2}\right) - \frac{i_L}{C_2}.u \end{cases} \qquad (5)$$

Table 1. MSX 60 solar panel specifications.

STC Power Rating (P_{mp})	60 W
Open Circuit Voltage (V_{oc})	21.1 V
Short Circuit Current (I_{sc})	3.8 A
Voltage at Maximum Power (V_{mp})	17.1 V
Current at Maximum Power (I_{mp})	3.5 A
Temperature coefficient of (V_{oc})	-0.08 V/°C
Temperature coefficient of (I_{sc})	0.003 %/°C

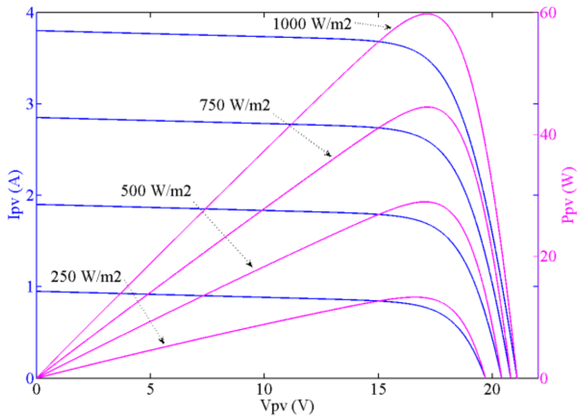

Fig. 2. PV power and current characteristics for different irradiances.

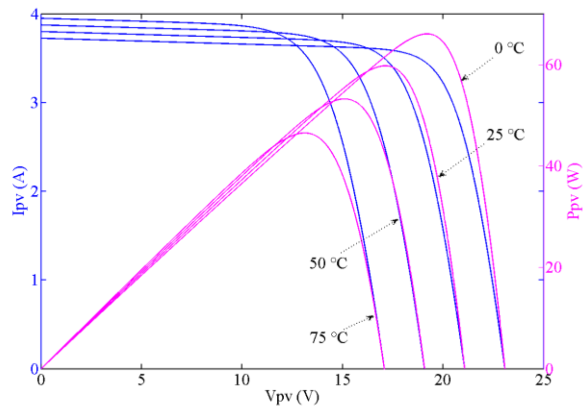

Fig. 3. PV power and current characteristics for different temperatures.

where i_L is the inductor current. The control input u is the switch position; it is set to 0 when the switch is open and it is set to 1 when the switch is closed.

If we set $x = [x_1 \quad x_2]^{Tr} = [i_L \quad V_0]^{Tr}$ with Tr matrix transpose, then the above expression can be written as:

$$\dot{x} = \frac{dx}{dt} = f(x,t) + g(x,t).u + h \qquad (6)$$

with $f(x) = \begin{bmatrix} 0 & \frac{-1}{L} \\ \frac{1}{C_2} & \frac{-1}{RC_2} \end{bmatrix}, g(x) = \begin{bmatrix} \frac{x_2}{L} \\ \frac{-x_1}{C_2} \end{bmatrix}, h = \begin{bmatrix} \frac{V_{pv}}{L} \\ 0 \end{bmatrix}$

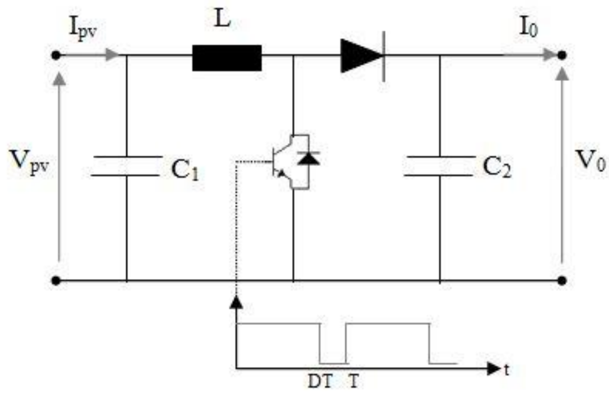

Fig. 4. DC-DC Boost converter topology.

4. MPPT TECHNIQUES

4.1 The perturb and observe method

The P&O method is most used in the literature and especially in practice because of its ease of implementation. It involves a perturbation in the PV array voltage or in the power converter duty ratio. Fig. 5 shows the flow chart of P&O method. It perturbs the PV output voltage periodically, and then it compares the PV output power with that of the previous cycle of perturbation. It can track the MPP but it has two main drawbacks; fluctuations around the peak power in normal operating conditions, poor convergence in the case of sudden variations in temperature and / or sunshine.

4.2 The Incremental conductance method

The IncCond follows the MPP by comparing the instantaneous conductance (I_{pv}/V_{pv}) with the incremental conductance (dI_{pv}/dV_{pv}) of the PV array (Radjai, 2014). At the MPP the two items are equal. Fig. 5 gives the flowchart of the IncCond method.

4.3 Improved sliding mode control method

The objective of the sliding mode control is firstly to design switching surface. Then, the second stage consists in conceiving a control law which is responsible to force the system trajectories towards this area of state space and will maintain it in this one (Bianconi, 2011). On sliding surface, the system has the desired behavior and is insensitive to parameter variations and external disturbances.

As shown in fig. 2 and fig. 3, when the PV panel is operating in its MPP, the slope of P-V characteristics is null

$$\frac{dP_{pv}}{dV_{pv}} = \frac{dV_{pv}\, I_{pv}}{dV_{pv}} = I_{pv} + V_{pv}\frac{dI_{pv}}{dV_{pv}} = 0 \qquad (7)$$

Then, the switching surface can be chosen as

$$S = \frac{dP_{pv}}{dV_{pv}} \qquad (8)$$

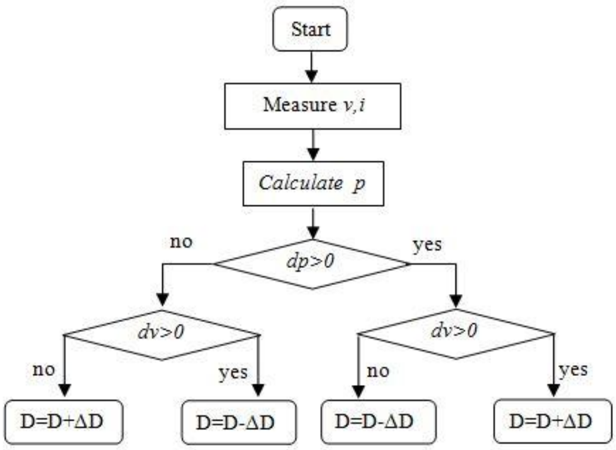

Fig. 5. Flowchart of the perturb and observe method

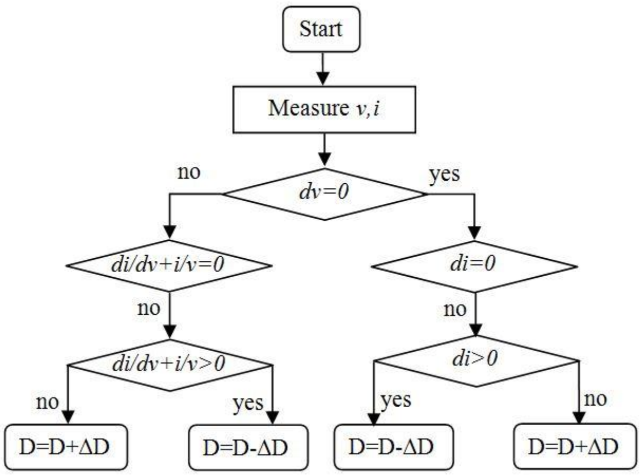

Fig. 6. Flowchart of the Incremental conductance method

The control law u of the converter is based on the fact that $S > 0$ on the left of the MPP and $S < 0$ on the right.

$$u = \begin{cases} 0 & if \quad S > 0 \\ 1 & if \quad S < 0 \end{cases} \tag{9}$$

When the sliding mode exists, the switching surface and its derivative will be nulls. The general control law u combine two terms, a non-linear component u_n and an equivalent control u_{eq}.

$$u = u_n + u_{eq} \tag{10}$$

These components determined by considering the Lyapunov function L satisfying the control objective both in attractively mode and in sliding mode.

$$L = \frac{1}{2} S(x)^2 \tag{11}$$

To ensure the attractiveness of the control variable to the switching surface, the time derivative of L must be negative definite.

$$L^{\dot{}} = S(x).\dot{S}(x) < 0 \ \forall\ S(x) \neq 0 \tag{12}$$

The latest expression is known under the name of reaching condition or stability condition.
In the ideal case and making some simplifying assumptions, the expression (1) becomes

$$I_{pv} = N_p\, I_{sc} - N_p\, I_{sc}\, exp\left(\frac{V_{pv}-V_{oc}}{n_s a\, v_t}\right) \tag{13}$$

And thus,

$$S(x) = I_{pv} + \frac{d[I_{pv}]}{dV_{pv}} V_{pv} = N_p\, I_{sc} - (N_p\, I_{sc} + \frac{N_p\, I_{sc}}{n_s a\, v_t} V_{pv})\, exp\left(\frac{V_{pv}-V_{oc}}{n_s a\, v_t}\right) \tag{14}$$

The derivative is given by:

$$\dot{S}(x) = -(2 + \frac{V_{pv}}{n_s a\, v_t}) \frac{N_p I_{sc}}{n_s a\, v_t}\, exp\left(\frac{V_{pv}-V_{oc}}{n_s a\, v_t}\right) \frac{dV_{pv}}{dt} \tag{15}$$

When $S(x) > 0$, the system operates on the left of the MPP, the voltage must be increased to attain the MPP ($\frac{dV_{pv}}{dt} > 0$), replacing in (15) it follows that $\dot{S}(x) < 0$, and hence $\dot{S}(x)S(x) < 0$.
When $S(x) < 0$, the system functions in right, the voltage must be decreased ($\frac{dV_{pv}}{dt} < 0$), which implies that $\dot{S}(x) > 0$, therefore $\dot{S}(x)S(x) < 0$.
Thus, the sliding mode exists and the system could reach global stability, regardless of the location of the operating point in left or in right of MPP.
To satisfy reaching condition (12), a constant rate reaching law can be selected to the non-linear component

$$u_n = -k_n.sgn(S(x)) \tag{16}$$

where k_n (positive constant), is the scaling factor which is tuned at the design time to adjust the step size.
The equivalent control u_{eq} proposed by Filippov (Slotine, 1991) characterize the system dynamics on the sliding surface, is determined by using the invariance conditions (Komurcugil, 2012):

$$S(x) = 0 \text{ and } \dot{S}(x) = 0 \tag{17}$$

$$\dot{S}(x) = \frac{dS(x)}{dt} = \left[\frac{\partial S}{\partial x}\right]^{Tr}.\dot{x} = \frac{\partial S}{\partial x_1}\dot{x_1} + \frac{\partial S}{\partial x_2}\dot{x_2} \tag{18}$$

From (14), it finds:

$$\frac{\partial S}{\partial x_2} = 0 \ \&\ \frac{\partial S}{\partial x_1} \neq 0 \tag{19}$$

Combination of formulas (17), (18) and (19), implies $\dot{x_1} = 0$, thus, we obtain:

$$u_{eq} = 1 - \frac{V_{pv}}{V_o} \tag{20}$$

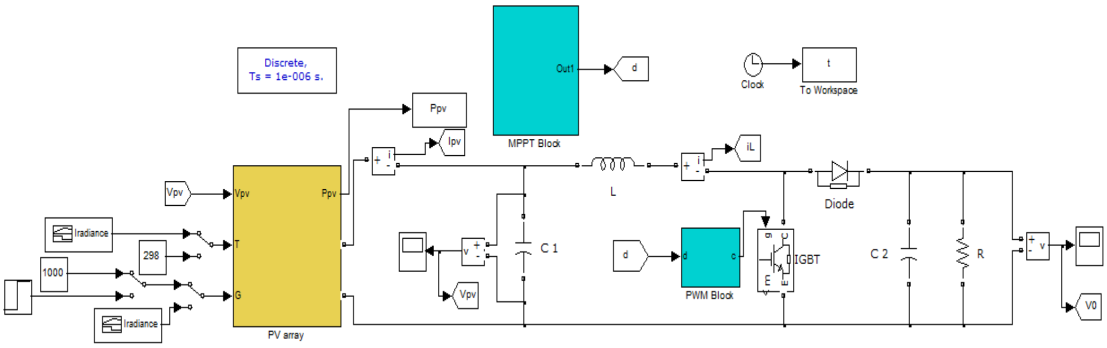

Fig. 7. Matlab/Simulink diagram of the photovoltaic system

After designing the sliding mode via the design of switching function and the reaching mode, it is then possible to express the overall control law by combining (16) and (20)

$$u = u_{eq} - k_n.sgn(S) \qquad (21)$$

This expression is applied when the operating point moves in the good direction towards the MPP, but if the operating point displaces far from the MPP the parameter k_n must be doubled. From this principle the method takes name of SMC with two different step sizes.

5. SIMULATION RESULTS

This study proposes a novel MPPT method to optimizing the yield of a photovoltaic module. The approach is based on sliding mode control with two different step sizes applied to Boost DC/DC converter as shown in fig. 7.

The work aims to verify the performance of the proposed MPPT tracker. The new method is compared to P&O and IncCond methods. A trapezoidal profile was chosen for varying irradiation between two levels from 500 W/m^2 (maximum power $P_{max} = 30\,W$, optimum voltage $V_{opt} = 8{,}55\,V$, optimum current $I_{opt} = 1{,}75\,A$) to 1000 W/m^2 (maximum power $P_{max} = 60\,W$, optimum voltage $V_{opt} = 17{,}1\,V$, optimum current $I_{opt} = 3{,}5\,A$) for a duration time of 1.2 s . All simulation tests are made using the switching frequency $\boldsymbol{f = 10\mathrm{kHz}}$ and the following parameters: $\boldsymbol{L = 0.5\mathrm{mH}}$, $\boldsymbol{C_1 = 1000\mu\mathrm{F}}$, $\boldsymbol{C_2 = 470\mu\mathrm{F}}$, $\boldsymbol{R = 30\Omega}$ and $\boldsymbol{T = 298\ \mathrm{Kelvin}}$.

The obtained simulation results for tracking MPP (maximum power, optimal current, optimal voltage) using P&O, IncCond and SMC are illustrated in fig. 8, fig. 9 and fig. 9, respectively. For example, one can read from fig. 10 at 0.7 second which correspond to standard test conditions (STC) the following values: maximum power $P_{max} = 59.6\,W$, optimum voltage $V_{opt} = 34{,}23 * \left(\frac{1}{2}V\right) = 17.115\,V$, optimum current $I_{opt} = 27{,}8 * \left(\frac{1}{8}A\right) = 3.475\,A$.

Fig. 11 depicts the comparison of tracking MPP between these three methods. It can be noticed that the P&O and the IncCond methods cannot track the true MPP especially when increasing or decreasing the irradiance. Fig. 12 compares the

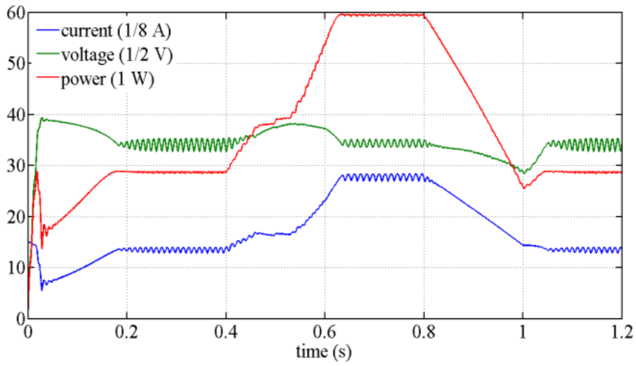

Fig. 8. Tracking MPP by using P&O method under a trapezoidal irradiation profile

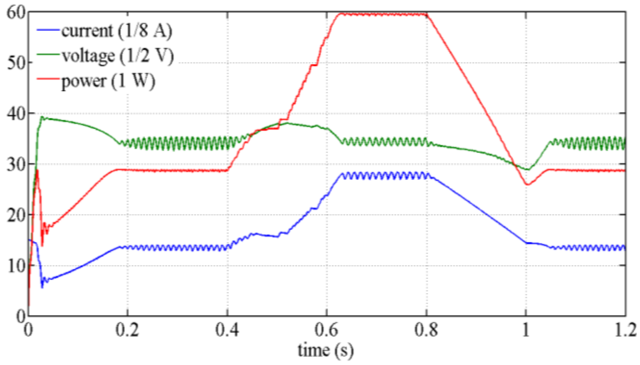

Fig. 9. Tracking MPP by using IncCond method under a trapezoidal irradiation profile

instantaneous efficiency between the new SMC, IncCond and P&O methods. The yield of PV panel by using the proposed algorithm is close to unity from 0.027 s until the end of the irradiance profile. At STC (irradiance of 1000 W/m^2, temperature of 25 °C), the MSX 60 module offers 60 W under optimal voltage value of 17.1 V and optimal current value of 3.5 A.

The results demonstrate that the current of MPP is dramatically affected by fast varying of irradiance, unlike to the MPP voltage which is only slightly affected. Also, it can be seen that the SMC approach has good dynamic response time at start-up; it is ten time faster than the two others methods. From figures of the simulation results, one can conclude that the proposed MPPT method has better performance compared to P&O and IncCond methods during both steady state and dynamic state conditions. In other terms, the proposed MPPT system can track the desired behavior of the maximum power rapidly and with fewer fluctuations which imply good conversion efficiency.

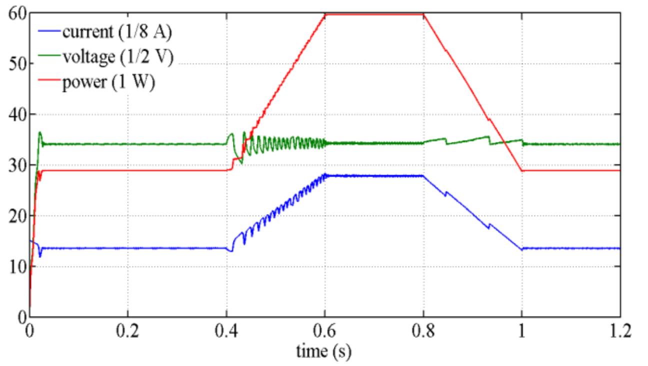

Fig. 10. Tracking MPP by using new SMC method under a trapezoidal irradiation profile

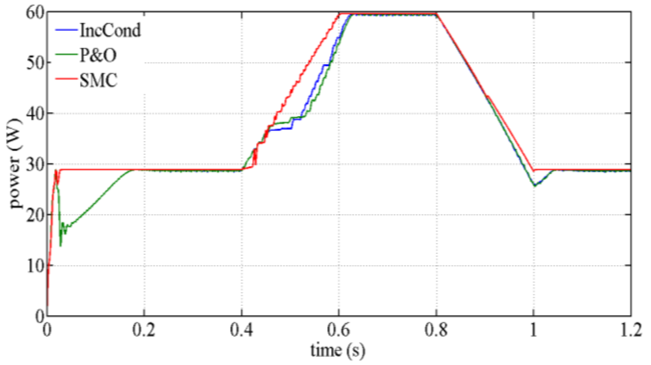

Fig. 11. Tracking MPP for the three methods under a trapezoidal irradiation profile

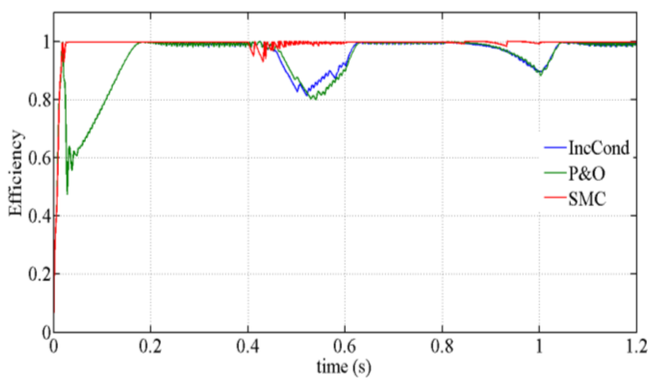

Fig. 12. Comparison of the instantaneous efficiency for the three methods under a trapezoidal irradiation profile

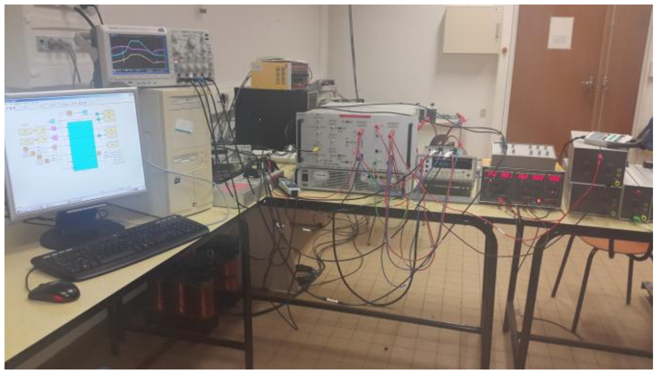

Fig. 13. Experimental test bench

6. EXPERIMENTAL RESULTS

An experimental model has been designed and built as shown in figure 13. The prototype which was built consists of a programmable DC voltage source (TDK-Lambda GEN 300-11) as an emulator which replaces the photovoltaic array, two diodes in order to block reverse currents in the PV source, DC/DC boost converter to step up the voltage level and resistance load. The LEM PR30 current probe is used in conjunction with Tektronix oscilloscope for measuring the PV output current. The differential sensor ST 1000 2-way is used to sense the input and output voltage of the converter. Operational Amplifiers are used to match the voltage levels of the variables being measured through the DSP Analog/Digital converter, which goes from 0 to 5V. The MPPT algorithms have been implemented in a DSP processor named DS1104 R&D controller board to generate the PWM signal for acting the IGBT gate of the boost converter. Control Desk software is used to supervise the displacement of the MPP on the P-V characteristics under constant or changing of climatic conditions.

Considering three MSX 60 modules connected in series feeds a resistance of 72 Ω, the temperature is kept fixe at 25 °C and the irradiance is changed with a trapezoidal profile between 500 W/m^2 and 1000 W/m^2. Figures 14, 15 and 16 show the waveforms of output current $\mathbf{I_{pv}(A)}$, voltage $\mathbf{V_{pv}(V)}$ and power $\mathbf{P_{pv}(W)}$ for the P&O, IncCond and SMC respectively. In fig. 16 one can see the oscillations in current and voltage curves. These oscillations are acceptable by the international norms because the ratio of their width to the average value is less than 5%. The experimental results confirm the results obtained by simulation. These results either in simulation or in experimental demonstrate that the SMC with two different step sizes is able to track the PV array MPP under constant or rapidly varying of irradiance with best performance in both steady and dynamic states compared to P&O and IncCond methods.

Using the Control Desk software, it can be draw Fig. 17, Fig. 18, Fig. 19. These figures present the practical behaviors of tracking maximum power point during the trapezoidal profile by using P&O, IncCond and modified SMC, respectively. They show the displacement of the peak power (MPP) when the irradiance profile change from 500 W/m^2 to 1000 W/m^2 (rising edge) and from 1000 W/m^2 to 500 W/m^2 (falling edge). The best method is that which takes a more rapid course. From the results, it can be concluded that the proposed MPPT present better performance in time response or in conversion efficiency than the P&O and IncCond methods.

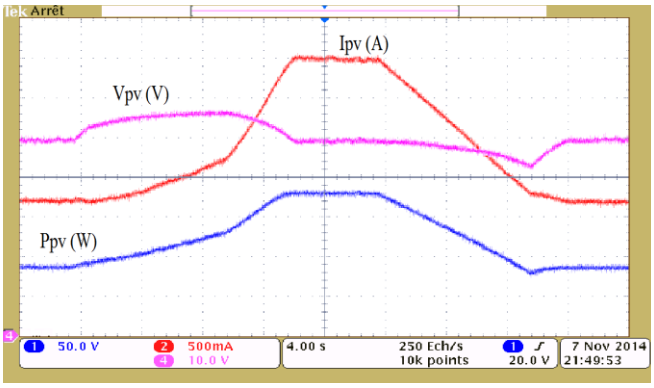

Fig. 14. Experimental measurement of the PV array power, voltage and current during a trapezoidal irradiation profile, using the P&O method (50 W/div, 500 mA/div, 10 V/div)

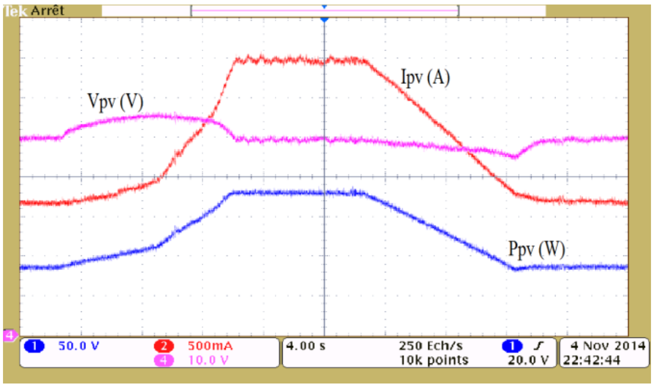

Fig. 15. Experimental measurement of the PV array power, voltage and current during a trapezoidal irradiation profile, using the modified IncCond method (50 W/div, 500 mA/div, 10 V/div)

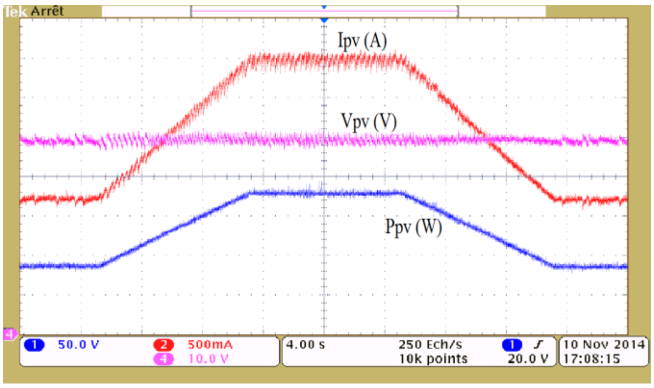

Fig. 16. Experimental measurement of the PV array power, voltage and current during a trapezoidal irradiation profile, using the modified IncCond method (50 W/div, 500 mA/div, 10 V/div)

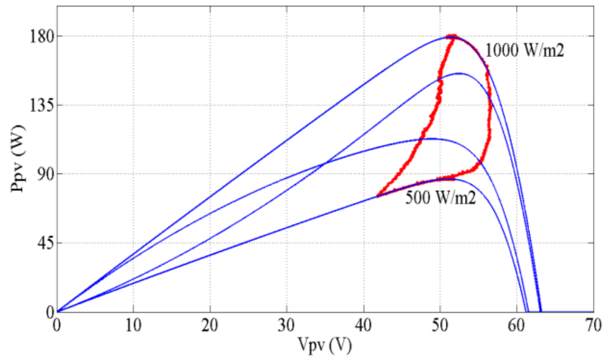

Fig. 17. Tracking of the PV peak power during a trapezoidal irradiation profile, using the P&O method

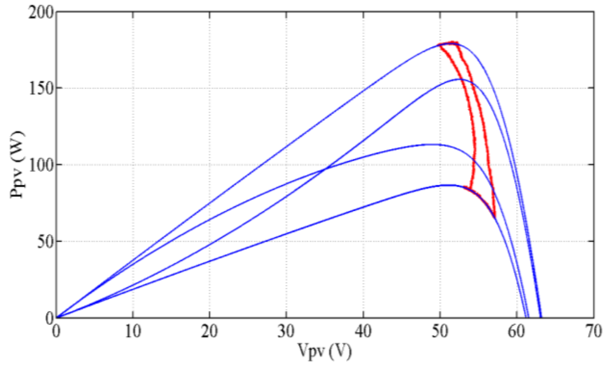

Fig. 18. Tracking of the PV peak power during a trapezoidal irradiation profile, using the IncCond method

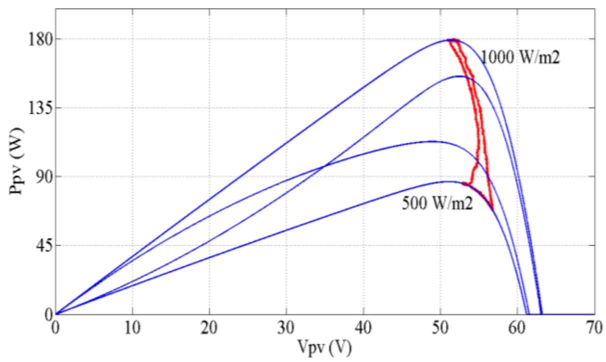

Fig. 19. Tracking of the PV peak power during a trapezoidal irradiation profile, using the proposed MPPT method

6. CONCLUSIONS

In this paper, a high performance MPPT based on sliding mode control applied to a boost converter has been presented. The proposed MPPT system by using two different step sizes is capable to track the maximum power under constant and fast changing of solar radiation conditions with best performance in both steady and dynamic states. The new MPP tracker has been compared to P&O and IncCond methods. It is designed, simulated and digitally implemented on the DS1104 R&D controller board**.** So, the aim of this work is attained and it can say that the proposed control technique may be considered as an interesting solution in PV Systems control area.

ACKNOWLEDGMENT

The work reported in this paper has been developed within the Laboratory of Information Technology and Automatic control for the Systems (LIAS), Poitiers University, France. And it has been supported by the CNEPRU research project No. J0201220110016, conducted at the department of electrical engineering, University of Setif, Algeria. This support is gratefully acknowledged.

REFERENCES

Ahmad H. Besheer, Ahmed M. Kassem, Almoataz Y. Abdelaziz, (2014), “Single-diode model based Photovoltaic module: Analysis and comparison approach”, *Electric Power Components and Systems*, 42:12, 1289-1300, doi: 10.1080/15325008.2014.927024.

Bianconi E., Calvente J., Giral R., Petrone G., Andres Ramos-Paja C., Spagnuolo G., Vitelli M., (2011),A fast current-based MPPT technique based on sliding mode control, *IEEE International Symposium on Industrial Electronics (ISIE)*, 27-30 June, Gdansk, Poland, pp. 59-64, doi: 10.1109/ISIE.2011.5984133.

Bianconi E., Calvente J., Giral R., Mamarelis E., Petrone G., Andres Ramos-Paja C., Spagnuolo G., Vitelli M., (2013), Perturb and observe MPPT algorithm with a current controller based on the sliding mode, *Electr. Power Energy Syst.* 44 (2013) 346-356, doi: 10.1016/j.ijeps.2012.07.046.

Dhar S., Sridhar R., Mathew G., (2013), Implementation of pv cell based standalone solar power system employing incremental conductance mppt algorithm, *IEEE International Conference on Circuits, Power and Computing Technologies (ICCPCT)*, 21st -23rd Mars 2013, Nagercoil, India, pp. 356-361, doi: 10.1109/ICCPCT.2013.6528926.

Esram, T., Chapman, P.L., (2007), Comparison of photovoltaic array maximum power point tracking techniques, *IEEE Trans. Energy Convers.*, 22, 2007, pp. 439–449

Femia N.,Petrone G.,Spagnuolo G.,Vitelli M., (2005), Optimization of perturb and observe maximum power point tracking method. *IEEE Transactions on Power Electronics*; 20 (4): 963–73.

Ghassami A.A., Sadeghzadeh S.M., Soleimani A., (2013), A high performance maximum power point tracker for PV Systems, *Electr. Power Energy Syst.* 53 (2013) 237-243, doi: 10.1016/j.ijeps.2013.04.017.

Kollimalla S.K., Mishra M.K., (2013), A new adaptive P&O MPPT algorithm based on FSCC method for photovoltaic system, *International Conference on Circuits, Power and Computing Technologies, ICCPCT*, 21st -23rd Mars 2013, Nagercoil, India, 406-411, doi: 10.1109/ICCPCT.2013.6529000.

Komurcugil H., (2012), Adaptive terminal sliding-mode control strategy for DC–DC buck converters, *ISA Transactions* No.51 (2012), pp.673-681, doi: 10.1016/j.isatra.2012.07.005.

Murtaza A.F., Sher H.A., Chiaberge M., Boero D., De Giuseppe M., Addoweesh K.E., (2012), A novel hybrid MPPT technique for solar PV applications using perturb & observe and fractional open circuit voltage techniques, 15th *International Symposium on Mechatronika*, 5th-7th December, Prague, Czech, pp. 1-8.

Pallavee Bhatnagar A. and Nema B. R. K., (2013), Conventional and global maximum power point tracking techniques in photovoltaic applications: A review, *j. renew. sustainable energy* 5, 032701 (2013), doi: 10.1063/1.4803524.

Petreus, D. ; Moga, D. ; Rusu, A. ; Patarau, T. ; Daraban, S., (2010), A Maximum Power Point tracker for photovoltaic system under changing luminosity conditions, 2010 *IEEE International symposium Industrial Electronics (ISIE)*, doi: 10.1109/ISIE.2010.5637829 , 2010 , Page(s): 556 – 561

Radjai T., Rahmani L., Mekhilef S., Gaubert J-P., (2014), “Implementation of a modified incremental conductance MPPT algorithm with direct control based on a fuzzy duty cycle change estimator using dSPACE”, *Solar Energy*, 110 (2014) 325-337, doi: 10.1016/j.solener.2014.09.014.

Ritesh Keshri, Manuele Bertoluzzo, Giuseppe Buja, (2014), Integration of a Photovoltaic panel with an electric city car, Electric Power Components and Systems, 42:5, 481-495, 2014, doi: 10.1080/15325008.2013.871374.

Salas, V., E. Olías, A. Barrado and A. Lázaro, (2006), Review of the maximum power point tracking algorithms for stand-alone photovoltaic systems. *Solar Energy Materials and Solar Cells*, 90, 1555-1578.

Safari, A., Mekhilef, S., (2011), Simulation and hardware implementation of incremental conductance MPPT with direct control method using cuk converter, *IEEE Trans. Ind. Electron.*, 2011, 58, pp. 1154–1161

Slotine J-J.E., Li W., (1991), *Applied Nonlinear Control*, (Prentice-Hall, Englewood Cliffs, New Jersey 07632, 1991), p.459.

Sotirios I. Nanou, Stavros A. Papathanassiou, (2014), Modeling of a PV system with grid code compatibility, *Electr. Power Syst. Res.* 116 (2014) 301-310, doi: 10.1016/j.epsr.2014.06.021.

Subudhi, B., Pradhan, R., (2012), A comparative study on maximum power point tracking techniques for photovoltaic power systems, *IEEE Trans. Sust. Energy*, 2012, pp. 89–98

Yu G.J., Jung Y.S., Choi J.Y., Kim G.S., (2004), A novel two-mode MPPT control algorithm based on comparative study of existing algorithms, *Sol. Energy* 76 (2004) 455-463, doi: 10.1016/j.solener.2003.08.038.

Xiao Weidong, Ozog Nathan, Dunford William G. (2007), Topology Study of Photovoltaic Interface for Maximum Power Point Tracking, *IEEE transactions on industrial electronics*, vol. 54, no. 3, june 2007, pp. 1696-1704.